

Perturbativity and mass scales of Left-Right Higgs bosons

Alessio Maiezza,^{1,*} Miha Nemevšek,^{2,†} and Fabrizio Nesti^{3,‡}

¹*IFIC, Universitat de València-CSIC, Apt. Correus 22085, E-46071 València, Spain*

²*Jožef Stefan Institute, Ljubljana, Slovenia*

³*Ruder Bošković Institute, Bijenička cesta 54, 10000, Zagreb, Croatia*

(Dated: March 15, 2016)

The scalar sector of the minimal Left-Right model at TeV scale is revisited in light of the large quartic coupling needed for a heavy flavor-changing scalar. The stability and perturbativity of the effective potential is discussed and merged with constraints from low-energy processes. Thus the perturbative level of the Left-Right scale is sharpened. Lower limits on the triplet scalars are also derived: the left-handed triplet is bounded by oblique parameters, while the doubly-charged right-handed component is limited by the $h \rightarrow \gamma\gamma, Z\gamma$ decays. Current constraints disfavor their detection as long as W_R is within the reach of the LHC.

PACS numbers: 12.60.Cn, 12.60.Fr, 12.15.Lk

I. INTRODUCTION

The standard model (SM) describes all the known particle interactions and their masses, except for the neutrino that is massless within the model, in contrast with the evidence of neutrino oscillations. An appealing solution is provided by the Left-Right symmetric model (LRSM) [1, 2], proposed to explain the most evident misfeature of the SM, that is the glaringly asymmetric chiral structure of the weak interactions. Incidentally, it has arisen as a complete theory for the origin of neutrino masses [3].

Left-Right theories possess a rich phenomenology, naturally embed the seesaw mechanism [3, 4] and, with the right-handed (RH) scale in the TeV region, provide a potentially dominant contribution to neutrino-less double beta decay ($0\nu 2\beta$) [5–7]. This contribution, due to the RH neutrino (N), could even be favored in the light of future cosmological bounds on the neutrino masses. Keung and Senjanović (KS) [8] proposed a low energy equivalent, where the heavy Majorana neutrino production could reveal LNV at colliders [9]. Recently, a complementary process [10] was analyzed at the LHC [11], looking for LNV in the SM-like Higgs decay.

The LRSM is based on the gauge group $\mathcal{G}_{LR} = SU(2)_L \times SU(2)_R \times U(1)_{B-L}$ plus either a generalized parity \mathcal{P} or charge conjugation \mathcal{C} [12]. The model is predictive in a number of ways: the Dirac neutrino coupling is univocally determined from the light and heavy neutrino mass [13], with direct consequences for LHC and for the electric dipole moment of the electron [13]. Moreover, in case of \mathcal{P} , the strong CP phase [14] and the quark flavor mixing in the RH sector are computable from the standard Cabibbo-Kobayashi-Maskawa matrix [15].

However, the TeV scale LRSM is non-trivially bounded by the low energy constraints, in particular $K^0 - \bar{K}^0$ and

$B_{d,s}^0 - \bar{B}_{d,s}^0$ oscillations [12, 16–19]. These, together with CP-violating processes, such as $\varepsilon', \varepsilon$ [20] and the electric dipole moment of the neutron [14], set a lower limit on the mass of the RH gauge boson $M_{W_R} > 2.9$ TeV. In the case of \mathcal{P} , the latter can set a substantial bound $M_{W_R} > 20$ TeV in case the strong CP problem is taken into account within the model [14].

Most of the above limits are in fact dominated by the tree-level exchange of flavor changing (FC) scalars [21], which have to be heavy. Their heavy masses require potentially large quartics that may become non-perturbative. This might be considered as a weak point of the minimal LRSM (see e.g. [22]), apparently spoiling the appeal of a predictive theory of neutrino masses.

The scalar potential of the LRSM with spontaneous parity breaking [2] has been the object of study from the original works to subsequent [23–27] and recent studies [28–30]. Nevertheless, a perturbativity analysis of the scalar potential was missing in literature until now. We provide this missing piece with a loop analysis and a renormalization of the Higgs sector. This leads to an effective potential and to a determination of the parameter space favored by perturbativity. In turn, it leads to a refined limit on the masses of W_R and the FC scalars. The entire analysis below holds for both the cases of \mathcal{P} and \mathcal{C} .

Furthermore, we assess the domain of perturbative regime for the mixing between the RH Higgs boson Δ_R^0 and the SM-like one, within the phenomenologically interesting region for collider searches [11].

Finally, the fairly large FC-scalar quartic also has an impact on oblique parameters and on the SM Higgs diphoton rate. These in turn set a lower bound on the left-handed triplet multiplet and the doubly charged component of the RH one. Therefore, an observation of W_R at the LHC would practically exclude the production of the entire left-handed triplet multiplet in the minimal LRSM. It would also allow for marginal space to observe the RH doubly charged component. On the other hand, the neutral RH Higgs remains fairly unconstrained and should be searched for at the LHC.

* amaiezza@ific.uv.es

† miha.nemevsek@ijs.si

‡ fabrizio.nesti@irb.hr

II. SCALAR POTENTIAL(S) AT TREE-LEVEL

The scalar content of the LRSM consists of a bi-doublet and two triplets

$$\phi = \begin{pmatrix} \phi_1^0 & \phi_2^+ \\ \phi_1^- & \phi_2^0 \end{pmatrix}, \quad \Delta_{L,R} = \begin{pmatrix} \frac{\Delta^+}{\sqrt{2}} & \Delta^{++} \\ \Delta^0 & -\frac{\Delta^+}{\sqrt{2}} \end{pmatrix}_{L,R}. \quad (1)$$

With the quantum number assignment $\phi \in (2_L, 2_R, 0)$, $\Delta_{L(R)} \in (3_L(1_L), 1_R(3_R), 2_{B-L})$ under \mathcal{G}_{LR} , the most general potential (\mathcal{V}) is constructed [2]. Since the basic feature of the LRSM is restoration of parity, an additional restriction is imposed on \mathcal{V} for the case of \mathcal{P} and \mathcal{C} . See Eqs. (A2) in the Appendix for the most general potentials.

Both gauge symmetry and LR parity are broken spontaneously (SSB) via the vev of the scalar fields

$$\begin{aligned} \langle \phi \rangle &= \begin{pmatrix} v_1 & 0 \\ 0 & v_2 e^{i\alpha} \end{pmatrix}, \\ \langle \Delta_L \rangle &= \begin{pmatrix} 0 & 0 \\ v_L e^{i\theta_L} & 0 \end{pmatrix}, \quad \langle \Delta_R \rangle = \begin{pmatrix} 0 & 0 \\ v_R & 0 \end{pmatrix}, \end{aligned} \quad (2)$$

where $v^2 \equiv v_1^2 + v_2^2 = 174$ GeV and $x \equiv \tan \beta = v_2/v_1 < 1$. Due to phenomenological constraints, the scales set by the vevs are fairly hierarchical $v_L \ll v \ll v_R$. For future convenience, it is useful to introduce the small parameter $\varepsilon = v/v_R$.

The symmetry breaking follows the pattern $\mathcal{G}_{LR} \xrightarrow{v_R} SU(2)_L \times U(1)_Y \xrightarrow{v_{1,2}} U(1)_{e.m.}$, and various masses are generated spontaneously. In particular, the gauge boson masses are

$$M_{W_R} \simeq g v_R, \quad M_W \simeq \frac{g v}{\sqrt{2}}. \quad (3)$$

In the following sections, we briefly review the minimization of the potential and the generation of the scalar mass spectrum of the LRSM.

A. Minimization of $\mathcal{V}_{\mathcal{P},\mathcal{C}}$

The minimization equations can be written as

$$\partial_{v_i} \mathcal{V} = 0, \quad (4)$$

for all $v_i \in \{v_1, v_2, v_R, v_L, \theta_L, \alpha\}$. In what follows, we stick to the \mathcal{P} potential. The case of \mathcal{C} follows straightforwardly and the results are summarized in the Appendix A.

The first three conditions in Eq. (4) provide μ_i^2 as a function of the vevs and the quartic couplings, shown in (A3)-(A5). The derivative on α provides a relation (A6) between the CP phases [24], which for small ε and x reads

$$2\alpha_2 \sin \delta_2 \simeq \alpha_3 x \sin \alpha. \quad (5)$$

Finally, derivation over v_L gives the well-know seesaw relation

$$v_L = \frac{\varepsilon^2 v_R}{(1+x^2)(2\rho_1 - \rho_3)} \left[\beta_1 x \cos(\alpha - \theta_L) + \beta_2 \cos(\theta_L) + \beta_3 x^2 \cos(2\alpha - \theta_L) \right]. \quad (6)$$

The phenomenology of neutrinos in the LRSM prevents v_L from taking a too large value

$$v_L < \frac{m_\nu}{m_N} v_R \simeq 10^{-5} \text{ GeV} \left(\frac{100 \text{ MeV}}{m_N} \right) \left(\frac{v_R}{10 \text{ TeV}} \right), \quad (7)$$

because $m_N \gtrsim 100$ MeV due to constraints from supernovae [31] and Big Bang nucleosynthesis [7], apart from the possible keV DM candidate [32].

This requires fairly small $\beta_i \lesssim 10^{-4}$, which are technically natural, both from fermion loops because of small neutrino Dirac masses, and from scalar loops since they are self-proportional. Even so, a stabilizing symmetry can be imposed [23, 25, 27] to guarantee a small v_L .

The remaining minimization condition on the derivative with respect to θ_L is automatically satisfied when $v_L \rightarrow 0$. In any case, for the purpose of this work β_i play no significant role, hence we drop them from here on.

B. Masses and physical states

Let us now construct the Hessian of \mathcal{V} and use the minimization solutions in (A3)-(A5) and (6). The positivity condition on the potential requires positive eigenvalues of the Hessian, which corresponds to positive squared masses of all the scalars. In this way, 8×8 , 4×4 and 2×2 matrices for squared masses of the neutral, singly and doubly charged fields are obtained.

At zero order ($\varepsilon, x \rightarrow 0$) these matrices are already diagonal. At higher orders in ε , subleading off-diagonal terms appear and one can solve the eigensystem perturbatively at given order, taking care of the would-be-Goldstone components. Δ_L decouples in the limit of $v_L \rightarrow 0$.

At first order in ε and $\mathcal{O}(x^2, \varepsilon x)$, we get the SM Higgs

$$h = \text{Re } \phi_1 + x \text{Re } \phi_2 - \theta \text{Re } \Delta_R^0, \quad (8)$$

with the EW mass

$$m_h^2 = \left(4\lambda_1 - \frac{\alpha_1^2}{\rho_1} \right) v^2, \quad (9)$$

and the mixing with the neutral component of $\text{Re } \Delta_R^0$ as¹

$$\theta = \varepsilon \frac{\alpha_1}{2\rho_1}. \quad (10)$$

¹ In phenomenological applications, the simplified 2×2 mass matrix with only h, Δ_R^0 is reliable in the $x \ll 1$ limit, e.g. as in [11]. In this case, the exact mixing parameter is $\tan(2\theta) = \frac{\alpha_1 v v_R}{\rho_1 v_R^2 - \lambda_1 v^2}$, from which the upper limit $|\theta| < \pi/4$ is clear.

	mass ² in v_R^2 units	states
H	$\alpha_3 + 4\varepsilon^2 \left(2\lambda_2 + \lambda_3 + \frac{4\alpha_2^2}{\alpha_3 - 4\rho_1} \right)$	$\text{Re } \phi_2 - x \text{Re } \phi_1$ $+\varepsilon \frac{4\alpha_2}{\alpha_3 - 4\rho_1} \text{Re } \Delta_R^0$
H'	$\alpha_3 + 9\varepsilon^2(\lambda_3 - 2\lambda_2)$	$\text{Im } \phi_2 + x \text{Im } \phi_1$
H^+	$\alpha_3 + \varepsilon^2 \frac{\alpha_3}{2}$	$\phi_2^+ + x \phi_1^+ + \frac{\varepsilon}{\sqrt{2}} \Delta_R^+$
Δ_R^0	$4\rho_1 + \varepsilon^2 \left(\frac{\alpha_1^2}{\rho_1} - \frac{16\alpha_2^2}{\alpha_3 - 4\rho_1} \right)$	$\text{Re } \Delta_R^0 + \varepsilon \frac{\alpha_1}{2\rho_1} \text{Re } \phi_1$ $-\varepsilon \frac{4\alpha_2}{\alpha_3 - 4\rho_1} \text{Re } \phi_2$
Δ_R^{++}	$4\rho_2 + \varepsilon^2 \alpha_3$	Δ_R^{++}
Δ_L^0	$\rho_3 - 2\rho_1$	$\text{Re } \Delta_L^0$ and $\text{Im } \Delta_L^0$
Δ_L^+	$\rho_3 - 2\rho_1 + \varepsilon^2 \frac{\alpha_3}{2}$	Δ_L^+
Δ_L^{++}	$\rho_3 - 2\rho_1 + \varepsilon^2 \alpha_3$	Δ_L^{++}

TABLE I. Masses and states in the LRSM (\mathcal{P}).

All the other scalars have the leading mass terms proportional to v_R with subleading electroweak corrections; the spectrum is shown in Table I. The same result holds for the case of \mathcal{C} , except for the masses of the FC scalars, quoted in the Appendix A, where the extra phases present in the potential cause modifications.

C. Flavor changing effects

The Yukawa couplings of H and H' to SM fermions lead to a non-diagonal Lagrangian in the flavor space [21].² As a consequence, FC processes such as meson oscillations, occur at tree-level and this sets the masses of $H(H')$ to be fairly heavy. A well known example is the one of $K^0 - \bar{K}^0$ mixing [12, 16–18] where H, H' and W_R , through the usual box diagrams, contribute to the process. As a result, the bound on the model manifests as a correlated constraint between M_{W_R} and $m_{H, H'}$.

Along this line, it was shown in [19] that constraints from $B_{d,s}^0 - \bar{B}_{d,s}^0$ are even more stringent than the ones from the Kaon sector, partially due to loop corrections to the tree-level FC contribution. From (3) and the leading masses of H, H' in Table I,

$$m_{H, H'} \simeq \sqrt{\alpha_3} v_R, \quad (11)$$

it is clear that a fairly large α_3 is required for a low RH scale to be compatible with B mixing. We incidentally

² A comment on possible FC effects of the SM-like Higgs boson is in order. The state shown in (8) leads to a diagonal Yukawa couplings in the Lagrangian, reproducing the SM. Expanding (8) to higher orders, FC effects occur because of small mixing with $H(H')$ of order $m_h^2/m_{H, H'}^2 \approx 10^{-5}$, however the related phenomenology is beyond current experimental search.

tally add that a sizeable x reduces α_3 for a given m_H in the above mass relation, but simultaneously increases the couplings to fermions, thus worsening the perturbativity of α_3 [12, 21]. In addition, it also increases the mixing of H with Δ_R^0 and further exacerbates the problem. Therefore we stick to $x \ll 1$ in what follows, the general case requires a dedicated study [33].

The size of α_3 can be approximated as a function of M_{W_R} as [19]

$$\alpha_3 \approx \frac{30}{(M_{W_R}/2.23 \text{ TeV})^2 - 1}. \quad (12)$$

This relation may generate a tension in the LRSM for low scale of M_{W_R} , where α_3 becomes large and potentially non-perturbative. Therefore, an evaluation of quantum corrections to the classical potential is in order, and we discuss it in the following section.

III. PERTURBATIVITY AND POTENTIAL AT QUANTUM LEVEL

An early discussion of perturbativity was presented already in [21], and a rough further estimate was made by [34] in the study of meson oscillations. The authors estimate the perturbative regime as $m_H < 10 M_{W_R}$. In order to update and clarify the perturbative status of the LRSM, we study the effective potential and focus on terms generated by the large α_3 . In subsection III A, we first renormalize the model and then build the effective potential. We compare the tree-level vertices with the one-loop correction in subsection III B, where perturbativity constraints on the relevant LRSM parameters emerge.

A. The effective potential

a. Renormalization. In order to construct the effective potential, one has to renormalize the theory with proper counter-terms. To illustrate the point, we first focus on the vertices related to Δ_R^0 and generalize to other ones below. For the present purpose, we demonstrate that only $\delta\mu_3$ and $\delta\rho_1$ need to be introduced

$$\mathcal{V}_{ct} = \delta\mu_3 \left[\Delta_R \Delta_R^\dagger \right] + \delta\rho_1 \left[\Delta_R \Delta_R^\dagger \right]^2, \quad (13)$$

where the trace is implied by the square parenthesis.

The following renormalization conditions are imposed:

- the tadpoles of Δ_R^0 vanish,
- the mass of Δ_R^0 remains the tree-level one.

This procedure ensures the finiteness of one loop contributions to any n -leg interaction of the scalars, delineating the effective potential. It also allows one to focus on interaction terms while keeping masses intact.

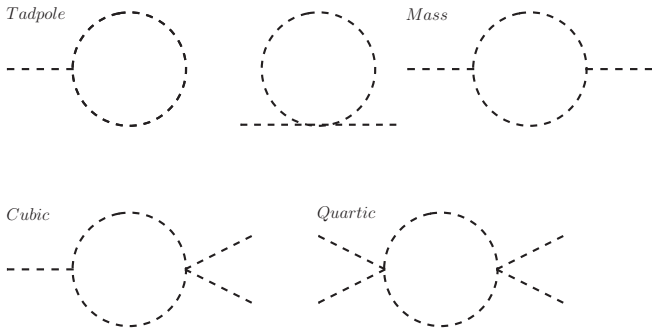


FIG. 1. Divergent diagrams that fix the counter-terms in Eq. (13).

Let us first focus on the divergent parts of diagrams in Fig. 1. It is enough to stick to the diagrams in which heavy scalars with mass dominated by α_3 are propagating. The generalization to the loops with the propagating Δ_R^0 is straightforward.

With the above renormalization conditions, the divergent parts of the tadpole and mass diagrams in Fig. 1 provide the equations

$$\delta_{\mu_3} - 2v_R^2 (\alpha_3^3 \Delta_\epsilon - \delta_{\rho_1}) = 0, \quad (14)$$

$$\delta_{\mu_3} - 2v_R^2 (\alpha_3^2 (\alpha_3 + 2) \Delta_\epsilon - 3\delta_{\rho_1}) = 0, \quad (15)$$

where the divergent part is defined as $\Delta_\epsilon = 16\pi^2 (2/\epsilon - \gamma + \log(4\pi))$. These equations fix the counterterms, i.e. $\delta_{\rho_1} = \alpha_3^2 \Delta_\epsilon$ and $\delta_{\mu_3} = 2\alpha_3^2 (\alpha_3 - 1) v_R^2 \Delta_\epsilon$. Simultaneously, the divergent part of the three-legs diagram in Fig. 1,

$$6i\sqrt{2}v_R (\alpha_3^2 \Delta_\epsilon - \delta_{\rho_1}), \quad (16)$$

vanishes when δ_{ρ_1} is inserted and leaves a finite result.

b. The effective potential. The finiteness holds for any number of external legs in the loop and all the finite parts can be formally summed as [35]

$$\mathcal{V}_{eff} = \mathcal{V} + \mathcal{V}_{ct} + \frac{1}{4} \sum_i \frac{m_i^4}{(4\pi)^2} \left[\log \left(\frac{m_i^2}{\mu^2} \right) - \frac{3}{2} \right], \quad (17)$$

where m_i^2 are the eigenvalues of the Hessian $\frac{\partial^2 \mathcal{V}}{\partial \phi_i \partial \phi_j}$ in the unbroken phase. Once the counter-terms are inserted in (17), a finite expression appears with μ -dependence in the constant part only.

Since we are interested in the effects of a large α_3 , we restrict the sum in Eq. (17) to Δ_R^0 and H, H' and H^\pm . Specifically, the relevant part for Δ_R^0 , that is the Higgs of the LRSM, can be expanded for small field values

$$\begin{aligned} \mathcal{V}_{eff} &= 4v_R^2 \rho_1 \Delta_R^0{}^2 \\ &+ \left[4\rho_1 + \frac{2}{(4\pi)^2} \left(\frac{4}{3} \alpha_3^2 + 18\rho_1^2 \right) \right] v_R \Delta_R^0{}^3 \\ &+ \left[\rho_1 + \frac{1}{(4\pi)^2} \left(\frac{8}{3} \alpha_3^2 + 27\rho_1^2 \right) \right] \Delta_R^0{}^4 + \mathcal{O}(\Delta_R^0{}^5). \end{aligned} \quad (18)$$

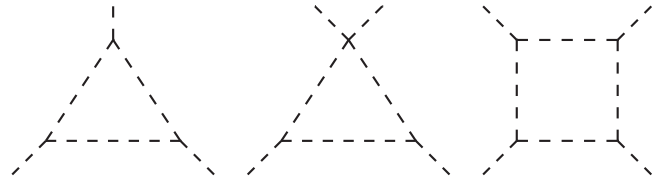


FIG. 2. Finite contributions to three and four legs scalar interactions that enter in the measure of perturbativity.

c. Stability. The quantum corrections in (18) may be dominated by α_3 , which also affects the stability of the potential. This assessment requires an expansion of Eq. (17) in the large field limit

$$\mathcal{V}_{eff} \approx \frac{1}{32\pi^2} \alpha_3^2 \Delta_R^0{}^4 \log \left(\frac{\Delta_R^0{}^2}{v_R^2} \right) > 0, \quad (19)$$

showing that stability is enhanced by the large α_3 .³

Incidentally, the sizeable α_3 contribution in the effective potential relaxes the destabilizing role of RH neutrinos [36], as described below.

B. Perturbativity constraints

In this section, we assess the level of perturbativity within the LRSM parameter space. Ultimately, one is interested in the mass scales of the theory, therefore we consider those parameters that are responsible for the leading mass contribution in Table I, in particular α_3 and also $\rho_{1,2,3}$.

We generalize the renormalization procedure outlined above, include the proper counterterms fixed by diagrams in Fig 1 and follow the same scheme. Each vertex of \mathcal{V}_{eff} will receive one loop contributions from many couplings, different from the tree-level one. This leads to correlated bounds, driven by vertices and suppressed by masses. We find that a reliable measure of perturbativity is given by purely self-induced corrections, computed by taking only one large coupling at the time. The dominant ones are four-leg vertices from Figs. 1 and 2, while the three-leg are less stringent. The ratio between the self-generated 1-loop and the corresponding tree-level parameter is then

³ In [37] an upper limit on α_3 was claimed from the requirement of boundedness of the classical potential. However, we note that the α_3 term in the scalar potential is positive definite, therefore no upper bound on α_3 can exist. We note that this result was used in a few subsequent works [38].

taken as a measure of perturbativity

$$\frac{\alpha_3^{(1)}}{\alpha_3} = \frac{3\alpha_3}{8\pi^2}, \quad (20)$$

$$\frac{\rho_1^{(1)}}{\rho_1} = \frac{27\rho_1}{16\pi^2}, \quad (21)$$

$$\frac{\rho_2^{(1)}}{\rho_2} = \frac{7\rho_2}{4\pi^2}, \quad (22)$$

$$\frac{\rho_3^{(1)}}{\rho_3} = \frac{3\rho_3}{16\pi^2}, \quad (23)$$

where the superscript (1) denotes the 1-loop value. Note that (21) reproduces the result from the effective potential in (18), as it should.

In addition to the quartics related to heavy scalars, one can generalize the discussion to the SM-like Higgs h . In particular, focusing on the λ_1 quartic, one gets

$$\frac{\lambda_1^{(1)}}{\lambda_1} = \frac{27\lambda_1}{16\pi^2}. \quad (24)$$

It should be kept in mind that when the actual physical processes (e.g. $\Delta_R^0 \Delta_R^0 HH$ scattering) are considered, the vertices of the interaction will typically be suppressed with respect to those in \mathcal{V}_{eff} . This is due to non-zero masses and momentum flowing in the loop. Both will regulate the loops and make the perturbative expansion more stable as the evaluation of the \mathcal{V}_{eff} .

In addition to perturbativity of the effective potential, one may consider requiring tree level unitarity of the scattering of LRSM scalars. The bounds from the optical theorem imply $\rho_{1,2} < 2\pi$, $\alpha_3, \rho_3 < 8\pi$. These are close or slightly more stringent than the ones from 100% perturbative level for $\rho_{1,2}, \alpha_3$, while for ρ_3 the unitarity bound matches with $\sim 50\%$ perturbativity.

IV. MASS SCALES IN TEV LRSM

The discussion in the previous section was independent of the LR scale, i.e. the perturbativity measure in Eqs. (20)-(23) are independent of M_{W_R} . Here we apply those results on the mass spectrum of the LRSM scalars.

In subsection IV A, we analyze the level of perturbativity for given masses of H and W_R , we then consider the mixing θ of the SM Higgs with Δ_R^0 in IV B, followed by limits on the RH neutrino from the stability of \mathcal{V}_{eff} in IV C. Finally, in subsections IV D and IV E, we deal with implications of α_3 on the mass of Δ_L due to oblique parameters and Δ_R^{++} via radiative Higgs decays to $\gamma\gamma(Z\gamma)$.

A. B mixing and W_R

The estimate of perturbativity and unitarity on α_3 from the previous section together with the B -oscillations limit

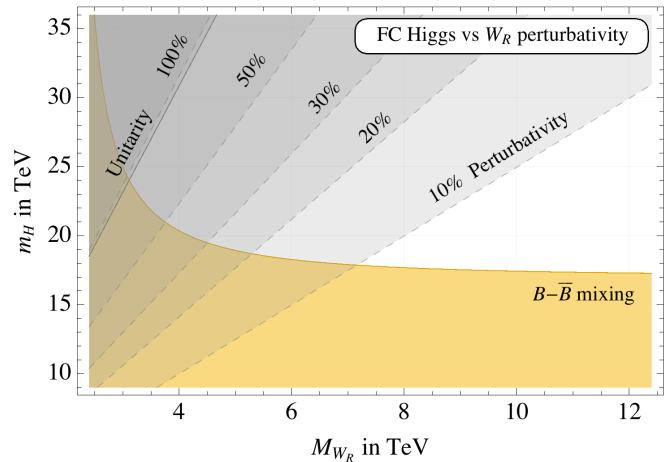


FIG. 3. Perturbativity assessment of \mathcal{V}_{eff} (dashed) and tree-level unitarity (solid) of α_3 , together with the bound on M_{W_R} vs. m_H from $B_{d,s}^0 - \bar{B}_{d,s}^0$ (see [19] for details).

in Eq. (12), impose a bound on M_{W_R} for a given perturbative level, as shown on Fig. 3. In [19] a rough evaluation of such bound for 100% perturbativity led to $M_{W_R} \gtrsim 3$ TeV. As clear from Fig. 3, the improved treatment basically confirms that result with a slight increase.

It is worth noting that the α_3 vertices from the scalar potential could directly affect the $B_{d,s}^0 - \bar{B}_{d,s}^0$ analysis after the renormalization of the H propagator as in the scheme of [34], where only gauge interactions were taken into account. The ensuing modification of Eq. (12) turns out to be $\sim 2\%$, therefore the B mixing bound remains reliable even with α_3 close to the unitarity bound.

B. Higgs mixing

Using the results of the previous section, one can understand the perturbative range of couplings relevant for the $h - \Delta_R^0$ Higgs mixing. In the physically interesting region $m_{\Delta_R^0} < \mathcal{O}(\text{TeV})$, its quartic ρ_1 is small and thus perturbative. As a result, α_1 also turns out to be small, for a given mixing angle, from (10). The point is then, that the correction to the mass of the Higgs in Eq. (9) becomes sizeable and needs to be canceled by a large λ_1 in order to preserve the light SM Higgs.

To a good approximation λ_1 can be determined for given $m_{\Delta_R^0}$ and θ as

$$4v^2\lambda_1 \simeq m_h^2 + \theta^2 m_{\Delta_R^0}^2, \quad (25)$$

which shows that with significant mixing θ , λ_1 becomes large for Δ_R^0 in the TeV range. At this point λ_1 may clash with Eq. (24), derived in the small α_1 limit, which translates into an upper bound on the mixing for a given Δ_R^0 mass, shown in Fig. 4. A considerable mixing is allowed for Δ_R^0 , whose mass can lie in the TeV range, still in perturbative regime.

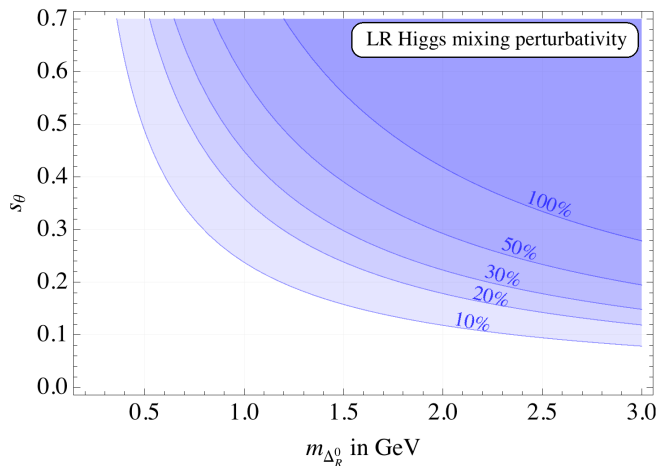


FIG. 4. Regions of Δ_R^0 -SM Higgs mixing s_θ favored by λ_1 perturbativity.

Notice that Higgs mixing will significantly affect electroweak processes and a stringent constraint on θ vs. the singlet mass was reported in [39]. However, the situation in the LRSM is more involved than the singlet case in [39] due to simultaneous presence of other sources (e.g. Δ_L below). A complete study would be in order, but lies beyond the scope of this paper.

C. Limit on the RH neutrino mass

As mentioned above, the sizeable α_3 contribution in the effective potential is positive, and this relaxes the destabilizing role of RH neutrinos. Their impact was considered in [36], where the role of quartics was not considered. Taking the RH neutrinos into account together with Eq. (19), we estimate

$$m_N \lesssim 2^{\frac{1}{4}} \sqrt{\alpha_3} v_R \simeq 1.85 M_{W_R} \sqrt{\alpha_3}, \quad (26)$$

where the gauge boson contribution is subleading and can be safely neglected. In fact, the B -mixing constraints imply the lower bound on α_3 as from Eq. (12). By considering this minimal required value of α_3 , we find that m_N below 25 TeV is allowed by stability, regardless of the LR scale.

The perturbativity upper bound on α_3 implies instead an absolute upper bound on m_N , depending on the required level of perturbativity. From (26) and using the upper values of α_3 from Eq. (20), we have

$$\frac{m_N}{M_{W_R}} \lesssim 2.3, 5.1, 7.3, \quad (27)$$

at 10, 50, 100% perturbativity, as shown on Fig. 5. It is clear that a quite heavy m_N is allowed, without ruining stability or perturbativity. This bound is further relaxed by the positive contributions of the other quartic couplings to \mathcal{V}_{eff} .

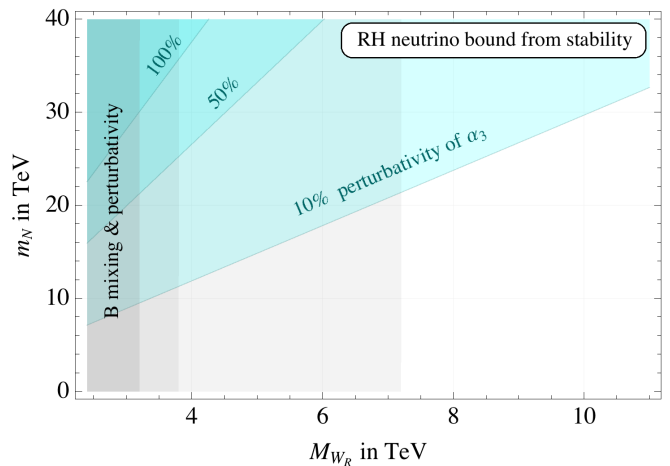


FIG. 5. An upper limit on m_N from the stability of the effective potential. The limit depends on α_3 , which in turn is perturbatively restricted (see text). The gray vertical bands correspond to regions disfavored by perturbativity at 10%, 50%, 100% (right to left) as from Fig. 3.

D. Oblique parameters and Δ_L

Oblique parameters, in particular the S and T , impose significant constraints on $SU(2)_L$ multiplets near the EW scale. The isospin violating T parameter is in principle sensitive to v_L and mass splittings within the Δ_L multiplet [23, 40]. However, due to the smallness of v_L (see Eq. (7)), only mass splittings are relevant.

In contrast to the stand-alone type II scenario, where the mass splitting is arbitrary, the embedding in the LRSM fixes the size and the sign of the spectrum. From Tab. I the following sum rule is obtained:

$$\frac{m_{\Delta_L^{++}}^2 - m_{\Delta_L^+}^2}{M_W^2} = \frac{m_{\Delta_L^+}^2 - m_{\Delta_L^0}^2}{M_W^2} = \left(\frac{m_H}{M_{W_R}} \right)^2 > 0, \quad (28)$$

which is quite robust, with corrections $\mathcal{O}(v_L/v)^2$.

The splitting in Eq. (28) is set by α_3 , which in turns depend on M_{W_R} , see Eq. (12). Therefore, at low scales, the LRSM requires sizeable mass splittings of Δ_L components. This has two significant implications:

1. The splitting of Δ_L components induces a large T parameter, that decouples when the entire multiplet is heavy, thus a lower bound emerges. The relevant oblique parameters are summarized in [41] and the global fit was performed in [42].

The resulting limit on Δ_L is shown on Fig. 6, where also the contribution of the θ mixing to S and T is taken into account. Clearly, the resulting bound on Δ_L is quite robust and in order to observe Δ_L at the LHC, a fairly large LR scale is required, beyond the reach of direct W_R searches.

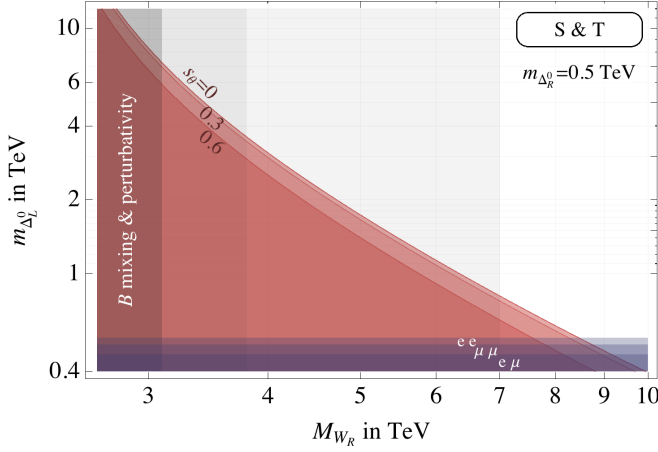


FIG. 6. Lower bound on the mass of the Δ_L multiplet, dominated by the large T parameter. The shaded regions are excluded at 2σ level for $s_\theta = (0, 0.3, 0.6)$ (upper to lower). The gray vertical bands correspond to regions disfavored by perturbativity at 10%, 50%, 100% (right to left) as from Fig. 3.

2. The charged components of Δ_L can be pair-produced at the LHC with masses up to about TeV [43]. Due to the small v_L (Eq. (7)) the di-gauge boson final state is suppressed.

When the mass splitting from Eq. (28) is larger than $\mathcal{O}(\text{GeV})$, the cascade decays $\Delta_L^{++} \rightarrow \Delta_L^+ W^{*+} \rightarrow \Delta_L^0 W^{*+} W^{*+}$ open up [40] and necessarily end up in Δ_L^0 due to the sum rule in Eq. (28). Since v_L is small, c.f. Eq. (7), the W^+W^- and $b\bar{b}$ final states are suppressed and the resulting final state is $\nu\bar{\nu}$, i.e. missing energy.

Ultimately, whether Δ_L^{++} decays via cascades or into same-sign lepton final state depends on the size of the heavy neutrino Majorana Yukawa coupling (see Fig. 1 in [40]).

One might wonder whether a fairly heavy Δ_L creates an additional perturbativity issue. However, it is clear from Eq. (23) that this is not the case. In fact, for $M_{W_R} \simeq 3$ TeV, even $m_{\Delta_L^0} \simeq 13$ TeV is consistent with $\sim 10\%$ level. Thus the region shown in Fig. 6 is perturbatively safe as far as ρ_3 is concerned.

E. Radiative Higgs decays and Δ_R^{++}

The α_3 coupling between the bi-doublet and triplets also induces loop processes with charged particles running in the loop. In particular, this affects the $h \rightarrow \gamma\gamma$ rate, whose coupling strength is measured by both ATLAS and CMS [44], while $h \rightarrow Z\gamma$ is yet to be seen [45].

The charged states that couple to the SM Higgs in the LRSM are W_R, H^+, Δ_L^+ and $\Delta_{L,R}^{++}$. The RH gauge

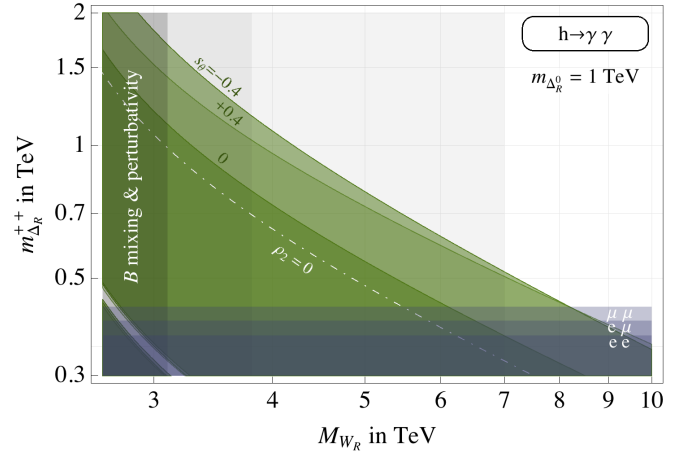


FIG. 7. Limit on the mass of Δ_R^{++} from the current data on $h \rightarrow \gamma\gamma$ [44]. The shaded green regions are ruled out at 2σ level and correspond to $s_\theta = (-0.4, 0.4, 0)$ (upper to lower). The gray vertical bands correspond to regions of perturbativity of 10%, 50%, 100% (right to left) as from Fig. 3. The lower blue bands correspond to direct searches for Δ_R^{++} [46] and are flavor dependent. The white strip in the lower left part is due to a cancellation with the SM. The region below the white dot-dashed line is where ρ_2 becomes negative and is disfavored by the boundedness of the classical potential.

boson contributions are suppressed due to heavy W_R and H^+ is too heavy to contribute, as clear from Table I. As discussed above, the entire Δ_L multiplet is also heavy, therefore the dominant contribution comes from Δ_R^{++} .

There are two contributing amplitudes in radiative channels. One comes from the direct coupling to h , the other from interference with Δ_R^0 through the mixing θ .

The amplitude is denoted as

$$\mathcal{A}^{\gamma\gamma} = \left(\frac{\alpha}{4\pi}\right) F((p_1 p_2)(\epsilon_1 \epsilon_2) - (\epsilon_1 p_2)(\epsilon_2 p_1)), \quad (29)$$

with $v = 2\sqrt{2}G_F$. Summing over photon polarizations and including the symmetry factor 1/2 leads to

$$\Gamma_{h \rightarrow \gamma\gamma} = |c_\theta F_h + s_\theta F_\Delta|^2 \left(\frac{\alpha}{4\pi}\right)^2 \frac{m_h^3}{64\pi}. \quad (30)$$

The dominant piece coming from Δ_R^{++} can be extracted from (B9) and one gets

$$F_h \simeq F_W + F_f + \sqrt{2}\alpha_3 v Q_{\Delta_R^{++}}^2 F_{\Delta_R^{++}}. \quad (31)$$

Current limit [44] on the Higgs $\gamma\gamma$ coupling strength requires the mass of Δ_R^{++} to be above few 100 GeV, depending on M_{W_R} and the Higgs mixing, as shown in Fig. 7. This constraint turns out to be more relevant than the direct pair-production searches and also overtakes the limit from the boundedness of the potential ($\rho_2 > 0$). It is also relevant for the collider vs. $0\nu 2\beta$ connection, since it constrains the rate mediated by W_R and Δ_R^{++} [6, 7].

The same scalar couplings also enter the $h \rightarrow Z\gamma$ loops. With the amplitude defined as

$$\mathcal{A}_h^{Z\gamma} = \frac{eg}{(4\pi)^2 c_w} G ((p_1 p_2) (\epsilon_1 \epsilon_2) - (\epsilon_1 p_2) (\epsilon_2 p_1)), \quad (32)$$

the decay rate turns out to be

$$\Gamma_{h \rightarrow Z\gamma} = |c_\theta G_h + s_\theta G_\Delta|^2 \left(\frac{\alpha}{4\pi} \right) \left(\frac{\alpha_2}{4\pi} \right) \frac{m_h^3}{32\pi c_w^2} \beta_{Zh}^3, \quad (33)$$

where $\beta_{Zh} = 1 - M_Z^2/m_h^2$ is the phase space suppression.

Current searches set a limit on the production cross-section around 10x the SM value [45]. This does not give any additional constraints on charged scalars; in fact even if the coupling strength limit were the same as $\gamma\gamma$, the $Z\gamma$ channel would still be less restrictive.

V. CONCLUSIONS

The minimal LRSM offers a predictive framework for the origin of neutrino masses and understanding parity violation of the electro-weak interactions. Because of its predictivity, several constraints emerge on the model. In particular, the masses of the FC scalars $H(H')$ have to be large and possibly lead to a tension in the parametric space of the low scale minimal LRSM. This may have a serious impact on the stability and perturbativity of the theory, which we address here.

We systematically study quantum corrections induced by large α_3 , responsible for the mass of H . After reviewing the potential, we perform the one-loop renormalization of the relevant part and build the effective potential.

As a first result, we show that the stability of the potential is improved thanks to the positive loop contribution of α_3 . This significantly relaxes the stability bound on the mass of the RH neutrino.

A reliable evaluation of the perturbative regime of the LRSM requires a study of the effective potential for all the relevant vertices. By focusing on those, we provide a simple conservative assessment of the regions of parameter space consistent with a given degree of perturbativity.

We translate the above bounds on coupling constants into constraints on physical scalar masses, which we bring together with the known flavor constraints on the LRSM. As a result, we find that a fairly light W_R is compatible with a perturbative effective potential.

Moreover, we study the mixing θ between the SM Higgs and Δ_R^0 , which is a sensitive probe of neutrino mass origin within the LRSM [11]. We conclude that a significant mixing is perturbatively safe for Δ_R^0 in the TeV range.

We also find that α_3 drives the oblique T parameter via Δ_L mass splitting. Therefore, a light W_R requires a large mass for the entire Δ_L , even in presence of Higgs mixing. We also ensure that this does not introduce an additional perturbativity problem related to the size of the relative quartics $\rho_{3,1}$.

Last but not least, a large α_3 modifies the $h \rightarrow \gamma\gamma$ decay rate, mainly through the Δ_R^{++} loop. In this way, present experimental constraints imply a correlated lower bound on $m_{\Delta_R^{++}}$ with M_{W_R} , which disfavors both of them to be easily accessible at the LHC, although some borderline space remains.

Notice that as far as the analysis performed in this paper is concerned, the same logic goes through in the model where two doublets [2] are considered instead of the usual triplets. Since the quark Yukawa sector is the same, it leads to a large FC Higgs mass that will have a similar issue with perturbativity. It will affect the oblique parameter in a similar way through the splitting of the components of the left-handed doublet and the right-handed singly charged Higgs will enter the $h \rightarrow \gamma\gamma$ loop in a similar fashion.

We conclude that a TeV scale W_R requires most of the scalar spectrum to be relatively heavy, apart from $m_{\Delta_R^0}$, which remains fairly unconstrained even in the presence of mixing.

ACKNOWLEDGMENTS

We thank S. Bertolini and G. Senjanović for useful discussions and reading the manuscript. MN would like to thank B. Bajc for an illuminating discussion. AM was supported in part by the Spanish Government and ERDF funds from the EU Commission [Grants No. FPA2011-23778, No. CSD2007-00042 (Consolider Project CPAN)] and by Generalitat Valenciana under Grant No. PROMETEOII/2013/007. MN was supported in part by the Slovenian Research Agency. FN was partially supported by the Croatian Science Foundation (HRZZ) project PhysMaB, "Physics of Standard Model and Beyond" as well as by the H2020 Twinning project No. 692194, "RBI-T-WINNING".

Appendix A: Potential(s)

The scalar potential is provided by all the possible bilinear and quartic terms of the scalar fields, obeying the gauge symmetry and a discrete LR symmetry, \mathcal{P} or \mathcal{C} .

Under \mathcal{P} , the scalars transform as

$$\mathcal{P} : \phi \rightarrow \phi^\dagger, \Delta_L \leftrightarrow \Delta_R \quad (A1)$$

and for the potential one has

$$\begin{aligned}
\mathcal{V}_{\mathcal{P}} = & -\mu_1^2 [\phi^\dagger \phi] - \mu_2^2 \left([\tilde{\phi} \phi^\dagger] + [\tilde{\phi}^\dagger \phi] \right) - \mu_3^2 \left([\Delta_L \Delta_L^\dagger] + [\Delta_R \Delta_R^\dagger] \right) \\
& + \lambda_1 [\phi^\dagger \phi]^2 + \lambda_2 \left([\tilde{\phi} \phi^\dagger]^2 + [\tilde{\phi}^\dagger \phi]^2 \right) + \lambda_3 [\tilde{\phi} \phi^\dagger] [\tilde{\phi}^\dagger \phi] + \lambda_4 [\phi^\dagger \phi] \left([\tilde{\phi} \phi^\dagger] + [\tilde{\phi}^\dagger \phi] \right) \\
& + \rho_1 \left([\Delta_L \Delta_L^\dagger]^2 + [\Delta_R \Delta_R^\dagger]^2 \right) + \rho_2 \left([\Delta_L \Delta_L] [\Delta_L^\dagger \Delta_L^\dagger] + [\Delta_R \Delta_R] [\Delta_R^\dagger \Delta_R^\dagger] \right) + \rho_3 [\Delta_L \Delta_L^\dagger] [\Delta_R \Delta_R^\dagger] \\
& + \rho_4 \left([\Delta_L \Delta_L] [\Delta_R^\dagger \Delta_R^\dagger] + [\Delta_L^\dagger \Delta_L^\dagger] [\Delta_R \Delta_R] \right) + \alpha_1 [\phi^\dagger \phi] \left([\Delta_L \Delta_L^\dagger] + [\Delta_R \Delta_R^\dagger] \right) \\
& + \alpha_2 e^{i\delta_2} \left([\tilde{\phi} \phi^\dagger] [\Delta_L \Delta_L^\dagger] + [\tilde{\phi}^\dagger \phi] [\Delta_R \Delta_R^\dagger] \right) + \text{h.c.} \\
& + \alpha_3 \left([\phi \phi^\dagger \Delta_L \Delta_L^\dagger] + [\phi^\dagger \phi \Delta_R \Delta_R^\dagger] \right) \\
& + \beta_1 \left([\phi \Delta_R \phi^\dagger \Delta_L^\dagger] + [\phi^\dagger \Delta_L \phi \Delta_R^\dagger] \right) + \beta_2 \left([\tilde{\phi} \Delta_R \phi^\dagger \Delta_L^\dagger] + [\tilde{\phi}^\dagger \Delta_L \phi \Delta_R^\dagger] \right) + \beta_3 \left([\phi \Delta_R \tilde{\phi}^\dagger \Delta_L^\dagger] + [\phi^\dagger \Delta_L \tilde{\phi} \Delta_R^\dagger] \right),
\end{aligned} \tag{A2}$$

where $\tilde{\phi} = \sigma_2 \phi^* \sigma_2$ and the square brackets imply the trace over field components.

From the minimization conditions in Eq. (4), the μ_i are computed in terms of vevs and the quartics

$$\begin{aligned}
\mu_1^2 = & \frac{2v_1^2 \lambda_1 (x^4 - 1) + 4v_1^2 \lambda_4 x (x^2 - 1) \cos(\alpha)}{x^2 - 1} \\
& + \frac{v_R^2 (\alpha_1 (x^2 - 1) + \alpha_3 x^2)}{x^2 - 1},
\end{aligned} \tag{A3}$$

$$\begin{aligned}
\mu_2^2 = & \sec(\alpha) \left[2v_1^2 \lambda_4 (x^2 + 1) \cos(\alpha) - \frac{\alpha_3 v_R^2 x}{2(x^2 - 1)} \right. \\
& \left. + 4v_1^2 \lambda_2 x \cos(2\alpha) + 2v_1^2 \lambda_3 x + \alpha_2 v_R^2 \cos(\alpha + \delta_2) \right]
\end{aligned} \tag{A4}$$

$$\begin{aligned}
\mu_3^2 = & 2\rho_1 v_R^2 + (\alpha_1 + (\alpha_1 + \alpha_3)x^2) v_1^2 \\
& + 4\alpha_2 x \cos(\alpha + \delta_2) v_1^2,
\end{aligned} \tag{A5}$$

where v_L is neglected, since $v_L \ll v \ll v_R$.

The derivative over α requires the relation between CP phases:

$$\sin(\delta_2) = \frac{x \sin(\alpha)}{2\alpha_2} \left[\frac{\alpha_3}{1 - x^2} - 4\epsilon^2 \frac{2\lambda_2 - \lambda_3}{1 + x^2} \right]. \tag{A6}$$

Alternatively, one can adopt the \mathcal{C} symmetry, which acts as

$$\mathcal{C} : \phi \rightarrow \phi^T, \quad \Delta_L \leftrightarrow \Delta_R^*. \tag{A7}$$

This choice allows for additional complex phases in the potential [28]. In particular, the couplings μ_2 , λ_2 , λ_4 , ρ_4 and β_i are now complex and one has to introduce a phase δ_c for each such coupling c . The same applies to the Yukawa sector leading to additional free phases in the RH CKM matrix [12, 15].

Again, the minimization conditions provide the μ_i pa-

rameters

$$\begin{aligned}
\mu_1^2 = & \frac{1}{x^2 - 1} \left[4v_1^2 \lambda_4 x (x^2 - 1) \cos(\alpha - \delta_{\lambda_4}) \right. \\
& \left. + 2v_1^2 \lambda_1 (x^4 - 1) + v_R^2 (\alpha_1 (x^2 - 1) + \alpha_3 x^2) \right],
\end{aligned} \tag{A8}$$

$$\begin{aligned}
\mu_2^2 = & \frac{\sec(\alpha - \delta_{\mu_2})}{2(x^2 - 1)} \left[(x^4 - 1) 2v_1^2 \lambda_4 \cos(\alpha - \delta_{\lambda_4}) \right. \\
& + 4v_1^2 x (x^2 - 1) (2\lambda_2 \cos(2\alpha - \delta_{\lambda_2}) + \lambda_3) \\
& \left. + 2\alpha_2 v_R^2 x^2 \cos(\alpha - \delta_2) (x^2 - 1) - \alpha_3 v_R^2 x \right],
\end{aligned} \tag{A9}$$

$$\begin{aligned}
\mu_3^2 = & 2\rho_1 v_R^2 + v_1^2 (\alpha_1 (1 + x^2) + \alpha_3 x^2) \\
& + 4\alpha_2 v_1^2 x \cos(\alpha - \delta_2),
\end{aligned} \tag{A10}$$

together with Equations analogous to (6) and (A6):

$$\begin{aligned}
v_L = & \epsilon^2 v_R \frac{\beta_1 x \cos(\alpha + \delta_{\beta_1} - \theta_L)}{(1 + x^2) (2\rho_1 - \rho_3)} \\
& + \frac{\beta_2 \cos(\delta_{\beta_2} - \theta_L) + \beta_3 x^2 \cos(2\alpha + \delta_{\beta_3} - \theta_L)}{(1 + x^2) (2\rho_1 - \rho_3)},
\end{aligned} \tag{A11}$$

$$\sin(\delta_2 - \delta_{\mu_2}) \simeq \frac{\alpha_3 x \sin(\alpha - \delta_{\mu_2})}{2\alpha_2 (x^2 - 1)}. \tag{A12}$$

The masses of the FC scalars in the case of \mathcal{C} are

$$m_{H(H')}^2 = v_R^2 \left[\alpha_3 + 8\epsilon^2 \left(\frac{\alpha_2^2 \pm \tilde{\alpha}}{\alpha_3 - 4\rho_1} + \frac{\lambda_3}{2} \right) \right], \tag{A13}$$

where

$$\begin{aligned}
\tilde{\alpha}^2 = & \alpha_2^4 + \lambda_2 (\alpha_3 - 4\rho_1) [\lambda_2 (\alpha_3 - 4\rho_1) + \\
& + 2\alpha_2^2 \cos(2\delta_2 - \delta_{\lambda_2})],
\end{aligned} \tag{A14}$$

and which reproduces the case of \mathcal{P} for vanishing extra-phases. A Left-Right potential with no $L \leftrightarrow R$ discrete symmetry was discussed in [28].

	Δ_R^{++}	$\Delta_L^{++}(\Delta_L^+)$	H^+
c_S^h	$\sqrt{2}(\alpha_1 + \alpha_3)$	$\sqrt{2}(\alpha_1 + \alpha_3)$	$2\sqrt{2}\lambda_1$
c_S^Δ	$2\sqrt{2}(\rho_1 + 2\rho_2)$	$\sqrt{2}\rho_3$	$\sqrt{2}(\alpha_1 + \alpha_3)$

TABLE II. Couplings of the LRSM Higgs bosons to charged scalars, relevant for radiative decays. S denotes the charged scalars $S = (\Delta_R^{++}, \Delta_L^{++}, \Delta_L^+, H^+)$.

Appendix B: Higgs decay loop functions

d. Higgs to $\gamma\gamma$. The SM contribution to the diphoton Higgs decay was computed some time ago [47]. The loop coefficients are

$$F_h = \sum_f N_f Q_f^2 F_f + F_W + \sum_S c_S^h v Q_S^2 F_S, \quad (\text{B1})$$

$$F_\Delta = F_{W_R} + \sum_S c_S^\Delta v_R Q_S^2 F_S, \quad (\text{B2})$$

and

$$F_f = -\frac{\sqrt{2}}{v} 2\beta_f [1 + (1 - \beta_f) f(\beta_f)], \quad (\text{B3})$$

$$F_W = \frac{\sqrt{2}}{v} [2 + 3\beta_W (1 + (2 - \beta_W) f(\beta_W))], \quad (\text{B4})$$

$$F_S = \frac{\beta_S}{m_S^2} [1 - \beta_S f(\beta_S)], \quad (\text{B5})$$

$$F_{W_R} = \frac{v}{v_R} F_W(\beta_{W_R}). \quad (\text{B6})$$

The corresponding dimensionless couplings $c_S^{h,\Delta}$ are obtained from the potential and are listed in Table II. The dimensionless f is the usual

$$f(\beta \geq 1) = \arcsin\left(\frac{1}{\sqrt{\beta}}\right)^2, \quad (\text{B7})$$

$$f(\beta < 1) = -\frac{1}{4} \left(\log\left(\frac{1 + \sqrt{1 - \beta}}{1 - \sqrt{1 - \beta}}\right) - i\pi \right)^2, \quad (\text{B8})$$

and $\beta_i = (2M_i/m_h)^2$. The scalar exchange part is

$$F_h + F_\Delta = (c_\theta c_S^h v + s_\theta c_S^\Delta v_R) Q_S^2 F_S \xrightarrow{\alpha_1 \rightarrow 0} \sqrt{2}\alpha_3 v Q_S^2 F_S. \quad (\text{B9})$$

This is typically the dominant new physics piece, since α_1 should not be too large for the theory to remain perturbative. For the same reason, we expect the second term in Eq. (B9) to be subdominant, also due to the mixing angle suppression.

e. Higgs to $Z\gamma$. The amplitude coefficients are

$$G_h = \sum_f N_f Q_f \hat{v}_f G_f + G_W + \sum_S c_S^h v Q_S \hat{v}_S G_S, \quad (\text{B10})$$

$$G_\Delta = G_{W_R} + \sum_S c_S^\Delta v_R Q_S \hat{v}_S G_S, \quad (\text{B11})$$

where $\hat{v}_f = T_{3L}/2 - Q_S^2 v_w$. The individual pieces are

$$G_f = \frac{2\sqrt{2}\beta\lambda}{v(\beta - \lambda)^2} \left[\beta - \lambda + ((\beta - 1)\lambda + \beta) \times (f(\beta) - f(\lambda)) - 2\beta(g(\lambda) - g(\beta)) \right], \quad (\text{B12})$$

$$G_W = \frac{\sqrt{2}c_w^2}{v(\beta - \lambda)^2} \left[(4 + 2(\beta - \lambda) - 3\beta\lambda)(\beta(1 + 2(g(\beta) - g(\lambda))) - \lambda) - \beta(f(\beta) - f(\lambda)) \times (\beta(3\lambda(\lambda + 2) - 8) + 2(2 - 3\lambda)\lambda) \right], \quad (\text{B13})$$

$$G_S = \frac{\beta\lambda}{m_S^2(\beta - \lambda)^2} \left[\lambda - \beta + \beta(\lambda(f(\lambda) - f(\beta)) + 2(g(\lambda) - g(\beta))) \right], \quad (\text{B14})$$

$$G_{W_R} = \frac{v}{v_R} G_W(\beta_{W_R}). \quad (\text{B15})$$

where

$$g(\beta \leq 1) = \sqrt{\beta - 1} \arcsin\left(\frac{1}{\sqrt{\beta}}\right), \quad (\text{B16})$$

$$g(\beta > 1) = \frac{\sqrt{1 - \beta}}{2} \left(\log\left(\frac{1 + \sqrt{1 - \beta}}{1 - \sqrt{1 - \beta}}\right) - i\pi \right). \quad (\text{B17})$$

In the $M_Z \rightarrow 0$ limit the F functions are recovered

$$G_i \xrightarrow{\lambda_i \rightarrow \infty} F_i. \quad (\text{B18})$$

[1] J.C. Pati and A. Salam, Phys. Rev. D **10**, 275 (1974) [Erratum-ibid. D **11**, 703 (1975)]; R.N. Mohapatra and

J.C. Pati, Phys. Rev. D **11**, 566 (1975); R.N. Mohapatra and J.C. Pati, Phys. Rev. D **11**, 2558 (1975).

- [2] G. Senjanović and R.N. Mohapatra, Phys. Rev. D **12**, 1502 (1975); G. Senjanović, Nucl. Phys. B **153**, 334 (1979).
- [3] R.N. Mohapatra, G. Senjanović, Phys. Rev. Lett. **44** (1980) 912.
- [4] P. Minkowski, Phys. Lett. B **67** (1977) 421.
- [5] R.N. Mohapatra and G. Senjanović, Phys. Rev. D **23** (1981) 165.
- [6] V. Tello, M. Nemevšek, F. Nesti, G. Senjanović and F. Vissani, Phys. Rev. Lett. **106** (2011) 151801 [arXiv:1011.3522 [hep-ph]].
- [7] M. Nemevšek, F. Nesti, G. Senjanović and V. Tello, [arXiv:1112.3061 [hep-ph]].
- [8] W.-Y. Keung, G. Senjanović, Phys. Rev. Lett. **50** (1983) 1427.
- [9] For a review, see: G. Senjanović, Int. J. Mod. Phys. A **26** (2011) 1469 [arXiv:1012.4104 [hep-ph]]; G. Senjanović, Riv. Nuovo Cim. **34** (2011) 1.
- [10] J.F. Gunion, B. Kayser, R.N. Mohapatra, N.G. Deshpande, J. Grifols, A. Mendez, F.I. Olness and P.B. Pal, PRINT-86-1324 (UC, DAVIS); J. F. Gunion, H. E. Haber, G. L. Kane and S. Dawson, Front. Phys. **80** (2000) 1.
- [11] A. Maiezza, M. Nemevšek and F. Nesti, Phys. Rev. Lett. **115** (2015) 081802 [arXiv:1503.06834 [hep-ph]].
- [12] A. Maiezza, M. Nemevšek, F. Nesti and G. Senjanović, Phys. Rev. D **82**, 055022 (2010) [arXiv:1005.5160 [hep-ph]].
- [13] M. Nemevšek, G. Senjanović and V. Tello, Phys. Rev. Lett. **110** (2013) 15, 151802 [arXiv:1211.2837 [hep-ph]].
- [14] A. Maiezza and M. Nemevšek, Phys. Rev. D **90** (2014) 9, 095002 [arXiv:1407.3678 [hep-ph]].
- [15] G. Senjanović and V. Tello, Phys. Rev. Lett. **114** (2015) 7, 071801 [arXiv:1408.3835 [hep-ph]], [arXiv:1502.05704 [hep-ph]].
- [16] G. Beall, M. Bander and A. Soni, Phys. Rev. Lett. **48** (1982) 848.
- [17] G. Ecker and W. Grimus, Nucl. Phys. B **258**, 328 (1985).
- [18] Y. Zhang, H. An, X. Ji and R.N. Mohapatra, Nucl. Phys. B **802**, 247 (2008) [arXiv:0712.4218 [hep-ph]].
- [19] S. Bertolini, A. Maiezza and F. Nesti, Phys. Rev. D **89** (2014) 9, 095028 [arXiv:1403.7112 [hep-ph]].
- [20] S. Bertolini, J.O. Eeg, A. Maiezza and F. Nesti, Phys. Rev. D **86** (2012) 095013 [arXiv:1206.0668 [hep-ph]]; S. Bertolini, A. Maiezza and F. Nesti, Phys. Rev. D **88** (2013) 3, 034014 [arXiv:1305.5739 [hep-ph]].
- [21] G. Senjanović and P. Senjanović, Phys. Rev. D **21**, 3253 (1980).
- [22] D. Guadagnoli and R. N. Mohapatra, Phys. Lett. B **694**, 386 (2011) [arXiv:1008.1074 [hep-ph]].
- [23] J. F. Gunion, J. Grifols, A. Mendez, B. Kayser and F. I. Olness, Phys. Rev. D **40** (1989) 1546.
- [24] K. Kierns, J. Kolb, J. Lee, A. Soni and G. H. Wu, Phys. Rev. D **66**, 095002 (2002) [hep-ph/0205082].
- [25] N. G. Deshpande, J. F. Gunion, B. Kayser and F. I. Olness, Phys. Rev. D **44** (1991) 837.
- [26] P. Duka, J. Gluza and M. Zralek, Annals Phys. **280** (2000) 336 [hep-ph/9910279].
- [27] O. Khasanov and G. Perez, Phys. Rev. D **65** (2002) 053007 [hep-ph/0108176]; K. Kierns, M. Assis and A. A. Petrov, Phys. Rev. D **71** (2005) 115015 [hep-ph/0503115]; K. Kierns, M. Assis, D. Simons, A. A. Petrov and A. Soni, Phys. Rev. D **73** (2006) 033009 [hep-ph/0510274].
- [28] W. Dekens and D. Boer, Nucl. Phys. B **889**, 727 (2014) [arXiv:1409.4052 [hep-ph]].
- [29] G. Bambhaniya, J. Chakraborty, J. Gluza, T. Jelinski and R. Szafron, Phys. Rev. D **92** (2015) 1, 015016 [arXiv:1504.03999 [hep-ph]].
- [30] P. S. B. Dev, R. N. Mohapatra and Y. Zhang, [arXiv:1602.05947 [hep-ph]].
- [31] R. Barbieri and R. N. Mohapatra, Phys. Rev. D **39** (1989) 1229.
- [32] M. Nemevšek, G. Senjanović and Y. Zhang, JCAP **1207** (2012) 006 [arXiv:1205.0844 [hep-ph]].
- [33] G. Senjanović, J. C. Vasquez, work in progress.
- [34] J. Basecq, L. F. Li and P. B. Pal, Phys. Rev. D **32**, 175 (1985).
- [35] M.E. Peskin and D.V. Schroeder, An Introduction To Quantum Field Theory (Frontiers in Physics).
- [36] R. N. Mohapatra, Phys. Rev. D **34** (1986) 909.
- [37] J. Chakraborty, P. Konar and T. Mondal, Phys. Rev. D **89** (2014) 5, 056014 [arXiv:1308.1291 [hep-ph]]. Phys. Rev. D **89** (2014) 9, 095008 [arXiv:1311.5666 [hep-ph]].
- [38] G. Bambhaniya, J. Chakraborty, J. Gluza, T. Jelinski and R. Szafron, Phys. Rev. D **92** (2015) 1, 015016 [arXiv:1504.03999 [hep-ph]]; A. Karam and K. Tamvakis, Phys. Rev. D **92** (2015) 7, 075010 [arXiv:1508.03031 [hep-ph]]; T. Mondal, U. K. Dey and P. Konar, Phys. Rev. D **92** (2015) 9, 096005 [arXiv:1508.04960 [hep-ph]]; N. Haba and Y. Yamaguchi, PTEP **2015** (2015) 9, 093B05 [arXiv:1504.05669 [hep-ph]].
- [39] A. Falkowski, C. Gross and O. Lebedev, JHEP **1505** (2015) 057 [arXiv:1502.01361 [hep-ph]]; S. I. Godunov, A. N. Rozanov, M. I. Vysotsky and E. V. Zhemchugov, Eur. Phys. J. C **76** (2016) 1, 1 doi:10.1140/epjc/s10052-015-3826-6 [arXiv:1503.01618 [hep-ph]].
- [40] A. Melfo, M. Nemevšek, F. Nesti, G. Senjanović and Y. Zhang, Phys. Rev. D **85** (2012) 055018 [arXiv:1108.4416 [hep-ph]].
- [41] L. Lavoura and L. F. Li, Phys. Rev. D **49** (1994) 1409 [hep-ph/9309262].
- [42] M. Baak *et al.* [Gfitter Group Collaboration], Eur. Phys. J. C **74** (2014) 3046 [arXiv:1407.3792 [hep-ph]].
- [43] G. Azuelos, K. Benslama and J. Ferland, J. Phys. G **32** (2006) 2, 73 [hep-ph/0503096].
- [44] The ATLAS and CMS Collaborations, ATLAS-CONF-2015-044.
- [45] S. Chatrchyan *et al.* [CMS Collaboration], Phys. Lett. B **726** (2013) 587 [arXiv:1307.5515 [hep-ex]].
- [46] G. Aad *et al.* [ATLAS Collaboration], JHEP **1503** (2015) 041 [arXiv:1412.0237 [hep-ex]].
- [47] J. R. Ellis, M. K. Gaillard and D. V. Nanopoulos, Nucl. Phys. B **106** (1976) 292; M. A. Shifman, A. I. Vainshtein, M. B. Voloshin and V. I. Zakharov, Sov. J. Nucl. Phys. **30** (1979) 711 [Yad. Fiz. **30** (1979) 1368]; W. J. Marciano, C. Zhang and S. Willenbrock, Phys. Rev. D **85** (2012) 013002 [arXiv:1109.5304 [hep-ph]].